

Electronic and Medium Effects on the Rate of Arene C–H Bond Activation by Cationic Ir(III) Complexes

David M. Tellers, Cathleen M. Yung, Bruce A. Arndtsen, Dan R. Adamson, and Robert G. Bergman*

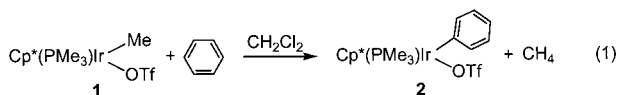
Contribution from the Division of Chemical Sciences, Lawrence Berkeley National Laboratory, and Center for New Directions in Synthesis, Department of Chemistry, University of California, Berkeley, California 94720

Received July 24, 2001

Abstract: A detailed mechanistic study of arene C–H activation in CH₂Cl₂ solution by Cp*(L)IrMe(X) [L = PMe₃, P(OMe)₃; X = OTf, (CH₂Cl₂)BAR_f; (BAR_f = B[3,5-C₆H₃(CF₃)₂)₄⁻] is presented. It was determined that triflate dissociation in Cp*(L)IrMe(OTf), to generate tight and/or solvent-separated ion pairs containing a cationic iridium complex, precedes C–H activation. Consistent with the ion-pair hypothesis, the rate of arene activation by Cp*(L)IrMe(OTf) is unaffected by added external triflate salts, but the rate is strongly dependent upon the medium. Thus the reactivity of Cp*(PMe₃)IrMe(OTf) can be increased by almost 3 orders of magnitude by addition of (*n*-Hex)₄NBAR_f, presumably because the added BAR_f anion exchanges with the OTf anion in the initially formed ion pair, transiently forming a cation/borate ion pair in solution (special salt effect). In contrast, addition of (*n*-Hex)₄NBAR_f to [Cp*PMe₃Ir(Me)CH₂Cl₂][BAR_f] does not affect the rate of benzene activation; here there is no initial covalent/ionic preequilibrium that can be perturbed with added (*n*-Hex)₄NBAR_f. An analysis of the reaction between Cp*(PMe₃)IrMe(OTf) and various substituted arenes demonstrated that electron-donating substituents on the arene increase the rate of the C–H activation reaction. The rate of C₆H₆ activation by [Cp*(PMe₃)Ir(Me)CH₂Cl₂][BAR_f] is substantially faster than [Cp*(P(OMe)₃)Ir(Me)CH₂Cl₂][BAR_f]. Density functional theory computations suggest that this is due to a less favorable preequilibrium for dissociation of the dichloromethane ligand in the trimethyl phosphite complex, rather than to a large electronic effect on the C–H oxidative addition transition state. Because of these combined effects, the overall rate of arene activation is increased by electron-donating substituents on both the substrate and the iridium complex.

Introduction

There is much interest in furthering our understanding of C–H bond breaking reactions because they hold great potential for developing new industrial processes and synthetic methodologies.^{1–3} In 1993 we reported an unusual iridium(III) complex, Cp*(PMe₃)IrMe(OTf) (**1**), that undergoes a mild and selective reaction with C–H bonds in arenes, alkanes, and other functionalized organic molecules (eq 1).⁴



We now wish to offer a more complete investigation of the mechanism of C–H bond activation by this compound, including a discussion of solvent and salt effects on the reaction rate

and the electronic character of the C–H activation transition state.^{5–9}

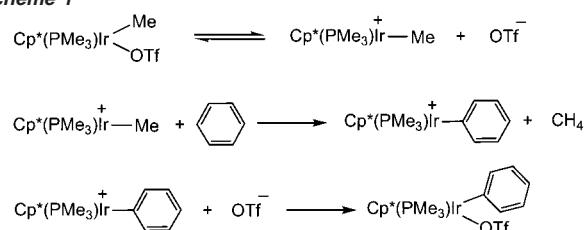
Complex **1** is both electronically and coordinatively saturated, yet it requires only mild conditions for benzene C–H activation (*t*_{1/2} = 2 h at 25 °C in CH₂Cl₂, eq 1). The mechanism of C–H activation with **1** continues to be the focus of current theoretical and experimental work.^{10–16}

Since mechanisms of C–H bond activation typically require a vacant coordination site on the metal, the simplest mechanistic

- (1) Arndtsen, B. A.; Bergman, R. G.; Mobely, T. A.; Peterson, T. H. *Acc. Chem. Res.* **1995**, *28*, 154.
- (2) Davies, J. A.; Watson, P. L.; Liebman, F.; Greenberg, A. *Selective Hydrocarbon Activation*; VCH: Toledo, 1990.
- (3) Stahl, S. S.; Labinger, J. A.; Bercaw, J. E. *Angew. Chem., Int. Ed.* **1998**, *37*, 2181.
- (4) Burger, P.; Bergman, R. G. *J. Am. Chem. Soc.* **1993**, *115*, 10462.

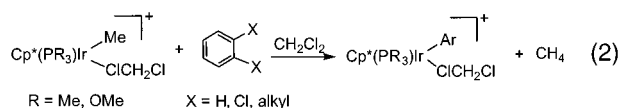
- (5) Tilset and co-workers have performed detailed experimental studies on related cationic platinum systems. See the four references immediately following this note.
- (6) Johansson, L.; Tilset, M. *J. Am. Chem. Soc.* **2001**, *123*, 739.
- (7) Heiberg, H.; Johansson, L.; Gropen, O.; Ryan, O. B.; Swang, O.; Tilset, M. *J. Am. Chem. Soc.* **2000**, *122*, 10831.
- (8) Johansson, L.; Tilset, M.; Labinger, J. A.; Bercaw, J. E. *J. Am. Chem. Soc.* **2000**, *122*, 10846.
- (9) Johansson, L.; Ryan, O. B.; Tilset, M. *J. Am. Chem. Soc.* **1999**, *121*, 1974.
- (10) Luecke, H. F.; Bergman, R. G. *J. Am. Chem. Soc.* **1998**, *120*, 11008.
- (11) Strout, D. L.; Zaric, S.; Niu, S.; Hall, M. B. *J. Am. Chem. Soc.* **1996**, *118*, 6068.
- (12) Su, M.-D.; Chu, S.-Y. *J. Am. Chem. Soc.* **1997**, *119*, 5373.
- (13) Hinderling, C.; Plattner, D. A.; Chen, P. *Angew. Chem., Int. Ed. Engl.* **1997**, *36*, 243.
- (14) Hinderling, C.; Feichtings, D.; Plattner, D. A.; Chen, P. *J. Am. Chem. Soc.* **1997**, *119*, 10793.
- (15) Alaimo, P. J.; Bergman, R. G. *Organometallics* **1999**, *18*, 2707.

Scheme 1



hypothesis for the reaction of saturated complex **1** involves prior dissociation of triflate, forming an unsaturated cationic 16e^- iridium fragment which then reacts to cleave the C–H bond (Scheme 1).

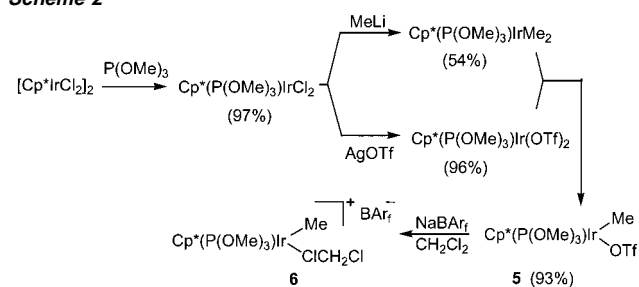
Consistent with this mechanism, it was shown that replacing the triflate ligand in **1** with the more weakly coordinating CH_2Cl_2 ligand and BAR_f [$\text{BAR}_f = \text{B}(3,5\text{-C}_6\text{H}_3(\text{CF}_3)_2)_4^-$] counterion increases the reactivity of the complex.¹⁷ The resulting compound **3** showed unprecedented reactivity, activating benzene at $-30\text{ }^\circ\text{C}$ (eq 2) to form $[\text{Cp}^*(\text{PMe}_3)\text{IrPh}(\text{CH}_2\text{Cl}_2)][\text{BAR}_f]$ (**4**).



Single-crystal X-ray analysis of **3** demonstrated that in the solid state, the borate anion is dissociated from the iridium fragment, with a chlorine-bound CH_2Cl_2 molecule occupying a coordination site on the metal center.

The quantitative mechanistic study of the reaction shown in eq 1 is complicated by the reaction's sensitivity to its environment. The study of medium effects in metal-mediated processes is an important but poorly understood area of chemistry.^{18–24} Solvent and salt effects in organic $\text{S}_{\text{N}}1$ reactions have been more extensively studied, but almost exclusively in relatively polar and/or protic solvents such as water, alcohols, and acetic acid. Adding an external salt usually increases the rate of such a dissociative reaction,^{25–30} in many cases by increasing the effective polarity of the medium. Reaction rate enhancement then occurs by a shift in an initial covalent/ionic dissociation equilibrium toward further dissociation at higher ionic strengths (the “normal salt effect”).³¹ Reactions that involve ionic dissociation in nonpolar solvents have been less extensively

Scheme 2



investigated and are less clearly understood. Phenomena such as the “common ion effect” are complicated when applied to nonpolar media, since ions created in these systems are likely to be highly associated and thus do not exist as free ions to any great extent. The possible presence of several associated ionic species (solvent-separated ion pairs, tight ion pairs, higher aggregates) complicates the mechanistic investigation of such processes.³¹

The studies discussed in this report were largely carried out on the reactions of iridium triflate **1** with arenes in dichloromethane solvent, both with and without added salts. In addition to the studies involving medium effects, we also examined the electronic requirements for Ir(III) aryl C–H bond activation. These effects were studied both via modification of the metal complex and by studying a range of disubstituted arenes. To facilitate these experiments, the phosphite analogue of **1**, $\text{Cp}^*(\text{P}(\text{OMe})_3)\text{IrMe}(\text{OTf})$ (**5**), was synthesized and investigated, as was the borate salt of this Ir(III) complex, $[\text{Cp}^*(\text{P}(\text{OMe})_3)\text{IrMe}(\text{CH}_2\text{Cl}_2)]^+[\text{BAR}_f]^-$ (**6**).

Results and Discussion

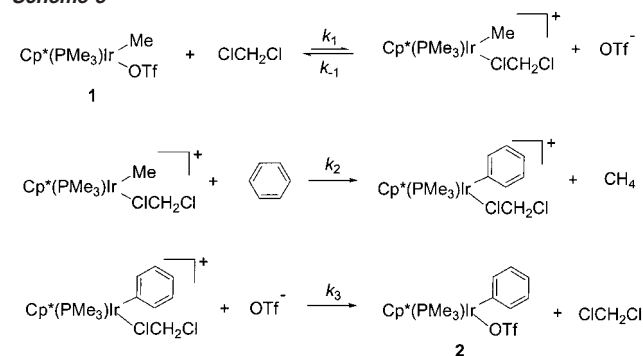
Synthesis of Compounds. The synthesis of the phosphite triflate complex **5** (Scheme 2) was accomplished by a route analogous to that used for the phosphine complex **1**.⁴ With $\text{Cp}^*(\text{P}(\text{OMe})_3)\text{IrMe}_2$, the reaction of 1 equiv of HOTf can be controlled to produce **5** as the major product. This is in contrast to $\text{Cp}^*(\text{PMe}_3)\text{IrMe}_2$, which more readily undergoes disubstitution, producing the corresponding bis-triflate complex. However, the conproportionation between $\text{Cp}^*(\text{P}(\text{OMe})_3)\text{IrMe}_2$ and $\text{Cp}^*(\text{P}(\text{OMe})_3)\text{Ir}(\text{OTf})_2$ (Scheme 2) was still the preferred synthetic route to the trimethyl phosphite complex **5**, since higher yields and cleaner initial products were obtained. Phosphite complex **5** does decompose slowly at room temperature, but it is more stable than the higher molecular weight iridium phosphites synthesized by Simpson, which readily decompose at room temperature by intramolecular C–H activation of the phosphite group.³² The phosphite borate complex **6** was generated via metathesis with NaBAR_f . It can be characterized in solution, but was found to be unstable when isolated both in the solid state and in solution at room temperature.

Kinetic Studies. Our first kinetic studies were carried out on the C–H activation reaction of benzene with trimethylphosphine-substituted methyl triflate **1** in dichloromethane solution. We considered the mechanism outlined in Scheme 3 (Scheme 4 for $\text{P}(\text{OMe})_3$) as a starting point for analysis of the data. With the knowledge that step 2 is irreversible, the rate law predicted for this mechanism is given in eqs 3 and 4, assuming the steady-

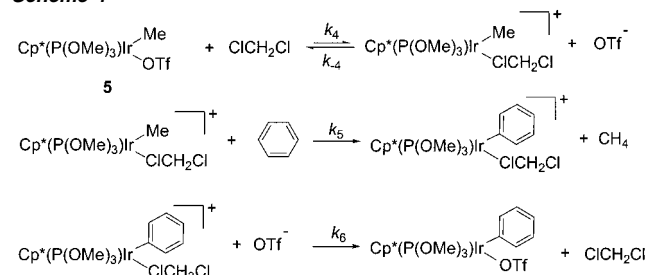
- (16) Klei, S. R.; Tilley, T. D.; Bergman, R. G. *J. Am. Chem. Soc.* **2000**, *122*, 1816.
 (17) Arndtsen, B. A.; Bergman, R. G. *Science* **1995**, *270*, 1970.
 (18) Castellani, M. P.; Hesse, E. T.; Tyler, D. R. *Organometallics* **1994**, *13*, 399.
 (19) Poli, R.; Owens, B. E.; Linck, R. G. *Inorg. Chem.* **1992**, *31*, 662.
 (20) Stahl, S. S.; Labinger, J. A.; Bercaw, J. E. *J. Am. Chem. Soc.* **1996**, *118*, 5961.
 (21) Trost, B. M.; Bunt, R. C. *J. Am. Chem. Soc.* **1998**, *120*, 70.
 (22) Brainard, R. L.; Nutt, W. R.; Lee, T. R.; Whitesides, G. M. *Organometallics* **1988**, *7*, 2379.
 (23) Peters, R. G.; White, S.; Roddick, D. M. *Organometallics* **1998**, *17*, 4493.
 (24) Cheng, T.; Brunschwig, B. S.; Bullock, R. M. *J. Am. Chem. Soc.* **1998**, *120*, 13121.
 (25) Allen, A. D.; Tidwell, T. T.; Tee, O. S. *J. Am. Chem. Soc.* **1993**, *115*, 10091.
 (26) Bockman, T. M.; Hubig, S. M.; Kochi, J. K. *J. Am. Chem. Soc.* **1998**, *120*, 2826.
 (27) Loupy, A.; Tchoubar, B.; Astruc, D. *Chem. Rev.* **1992**, *92*, 1141.
 (28) Hossain, M. A.; Schneider, H. *Chem.-Eur. J.* **1999**, *5*, 1284.
 (29) Winstein, S.; Klinedinst, P. E.; Robinson, G. C. *J. Am. Chem. Soc.* **1961**, *83*, 885.
 (30) Goodson, F. E.; Wallow, T. I.; Novak, B. M. *J. Am. Chem. Soc.* **1997**, *119*, 12441.
 (31) Loupy, A.; Tchoubar, B. *Salt Effects in Organic and Organometallic Chemistry*; VCH: Weinheim, Germany, 1992; Chapter 2.

- (32) Simpson, R. D. *Organometallics* **1997**, *16*, 1797.

Scheme 3



Scheme 4



state approximation and a fast, essentially complete final recombination step.

$$\text{rate} = k_{\text{obs}}[\mathbf{1}] = \frac{k_1 k_2 [\text{C}_6\text{H}_6]}{k_{-1} [\text{OTf}] + k_2 [\text{C}_6\text{H}_6]} \quad (3)$$

$$\text{rate} = k_{\text{obs}}[\mathbf{5}] = \frac{k_4 k_5 [\text{C}_6\text{H}_6]}{k_{-4} [\text{OTf}] + k_5 [\text{C}_6\text{H}_6]} \quad (4)$$

At sufficiently high benzene concentrations, we would predict saturation behavior in arene for this mechanism ($k_{\text{obs}} = k_1$ at high R–H concentrations). However, complex **1** does not show this saturation behavior at elevated benzene concentrations in dichloromethane at 10 °C (Figure 1). While the reaction rate does increase as expected at low benzene concentrations, it actually *decreases* at benzene concentrations greater than 3 M. We believe this is because at these very high concentrations of benzene, the effective polarity of the solvent is perturbed, becoming substantially less polar than pure CH_2Cl_2 . This would shift the initial ionization equilibrium toward the covalent complex **1** (Scheme 3), inhibiting the overall rate. At the suggestion of a referee, at 2.6 M benzene concentration cyclohexane- d_{12} , instead of additional benzene, was added to the reaction mixture to determine whether this would produce rate retardation similar to that observed at higher concentrations of benzene. The k_{obs} without added C_6D_{12} was measured to be $2.32 \times 10^{-4} \text{ s}^{-1}$ (2.6 M C_6H_6 , 10 °C). When 0.5 and 1.0 M C_6D_{12} were added, the reaction rates were measured to be 1.43×10^{-4} and $9.59 \times 10^{-5} \text{ s}^{-1}$, respectively. Addition of C_6D_{12} to the reaction mixture thus decreases the k_{obs} , supporting our explanation of the decrease in rate observed at high benzene concentrations. In addition, a $\text{C}_6\text{H}_6/\text{C}_6\text{D}_6$ isotope effect of 3.5 was measured at 1.0 M benzene concentration, demonstrating that kinetic saturation in $[\text{C}_6\text{H}_6]$ is not achievable under these conditions with complex **1**. At substrate saturation, there should be little or no isotope effect observed, since the rate would be substrate independent and would only depend on k_1 .

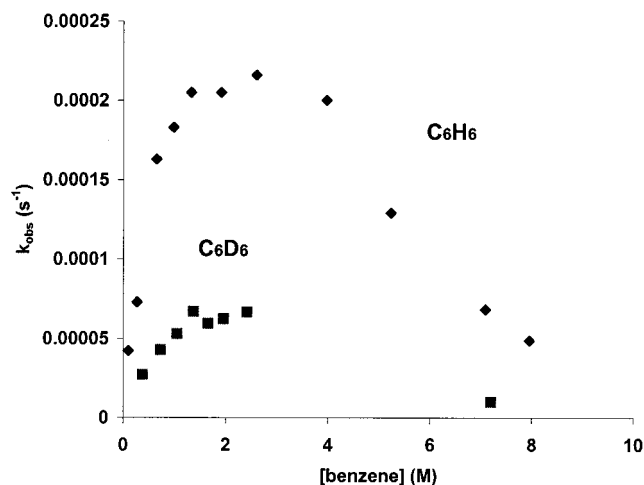


Figure 1. Plot of observed rate constant (k_{obs}) vs $[\text{C}_6\text{H}_6]$ and $[\text{C}_6\text{D}_6]$ for the reaction of **1** (1.1 mM) at 10 °C. PPNOTf (1.8 mM) was also present.

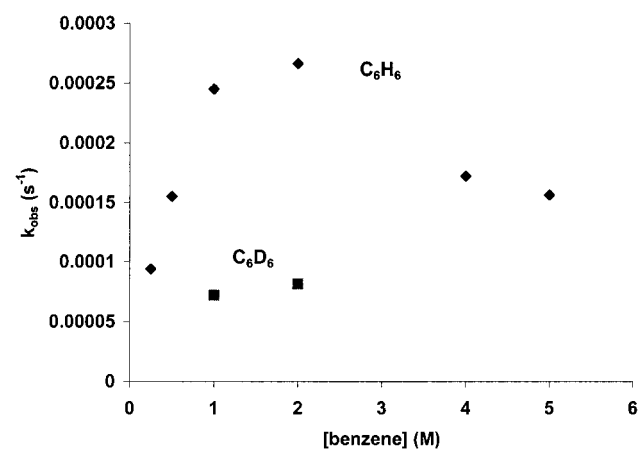


Figure 2. Plot of observed rate constant (k_{obs}) vs $[\text{C}_6\text{H}_6]$ and $[\text{C}_6\text{D}_6]$ for the reaction of **5** (12.0 mM) at 30 °C.

A similar result was obtained when the phosphite triflate complex **5** was treated with varying amounts of benzene in dichloromethane at 30 °C (Figure 2). The reaction rate begins to decrease at concentrations greater than 2 M, and an isotope effect ($\text{C}_6\text{H}_6/\text{C}_6\text{D}_6$, 1.0 M benzene concentration) of 3.6 is observed. In addition, the overall rate of reaction of **5** with benzene is substantially slower than that for **1**. We suggest that this result is due to the fact that P(OMe)_3 is more electron-withdrawing than PMe_3 , slowing the initial triflate dissociation step (k_4) in the phosphite complex **5** (vide infra) (Scheme 4).

Salt Concentration Dependence on the Reactivity of 1, 3, and 5. To probe the effect of ionic strength on the C–H activation reaction, the reaction of the triflate complex **1** with benzene in dichloromethane was run in the presence of variable amounts of $[(\text{PPh}_3)_2\text{N}][\text{B}(3,5\text{-C}_6\text{H}_3(\text{CF}_3)_2)_4]$ (PPNBARf). At higher $[\text{PPNBARf}]$ (>20 mM), the kinetic analysis was complicated by the rapid formation of PPNOTf as a precipitate during the reaction. Thus the triflate complex **1** not only reacted with benzene but also simultaneously underwent a metathesis reaction, to generate the more reactive CH_2Cl_2 /borate complex **3** (Scheme 5).

The reaction of the methyl triflate complex **1** with PPNBARf without benzene present was shown by NMR analysis to also proceed within minutes to the CH_2Cl_2 /borate complex **3**. Similarly, the phenyl triflate complex **2** reacts with PPNBARf

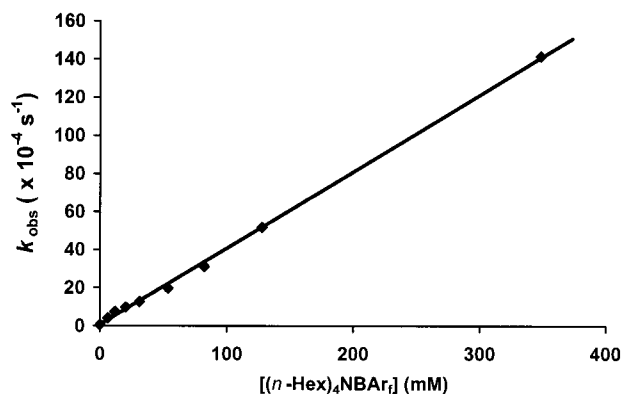
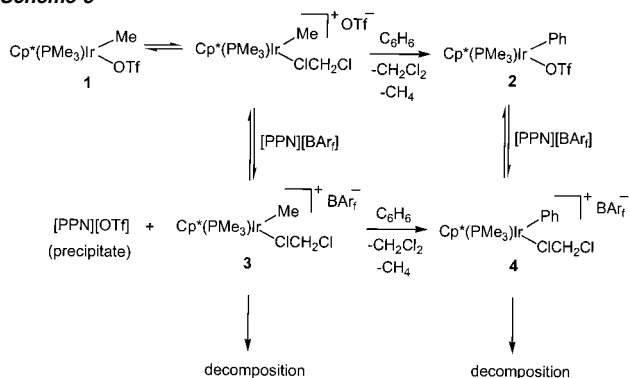


Figure 3. Plot of observed rate constant (k_{obs}) vs $[(n\text{-Hex})_4\text{NBAR}_f]$ for the reaction of **1** (1.90 mM) and C_6H_6 (51.2 mM) at 25.2 °C in CH_2Cl_2 .

Scheme 5



to form the less stable phenyl CH_2Cl_2 /borate complex **4**. A summary of the reactions of **1** with PPNBAR_f and benzene in dichloromethane is shown in Scheme 5.

This metathesis, precipitation, and decomposition behavior prevented us from collecting reliable kinetic data in the presence of PPNBAR_f . To circumvent these problems, a more hydrophobic salt, $(n\text{-Hex})_4\text{NBAR}_f$, was used. In this case no precipitate is observed, and we believe that with $(n\text{-Hex})_4\text{NBAR}_f$, neither the methyl triflate complex **1** nor the phenyl triflate complex **2** undergoes extensive metathesis to form the corresponding CH_2Cl_2 /borate complexes at room temperature (i.e., the position of the equilibrium strongly favors the covalent iridium triflate complex **1**). The reaction of **1** with benzene using variable concentrations of $(n\text{-Hex})_4\text{NBAR}_f$ proceeds cleanly even at extremely high $(n\text{-Hex})_4\text{NBAR}_f$ concentrations (up to 350 mM). The plot of k_{obs} versus $[(n\text{-Hex})_4\text{NBAR}_f]$ is shown in Figure 3. The added salt strongly accelerates the rate, and the plot is linear over a wide range of $(n\text{-Hex})_4\text{NBAR}_f$ concentrations.

Similar behavior is observed when the reaction of phosphite triflate complex **5** with benzene is run in the presence of variable concentrations of $(n\text{-Hex})_4\text{NBAR}_f$ (Figure 4). At relatively low salt concentrations (<200 mM), the reaction rate increased linearly with the concentration of salt. At higher salt concentrations, the reaction rate still increased, but began to deviate from linear behavior. The reaction rate could not be measured with accuracy at high salt concentrations (>400 mM), because the solubility limit of the salt in CH_2Cl_2 was reached.³³ The reaction rate for both **1** and **5** in the presence of added $(n\text{-Hex})_4\text{NBAR}_f$

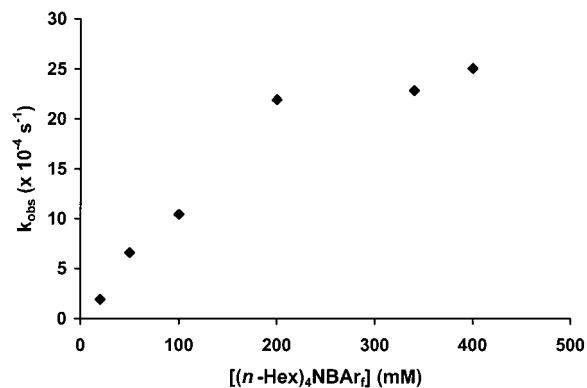
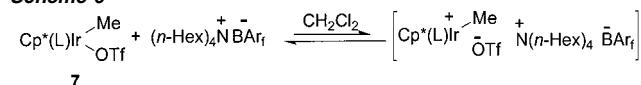
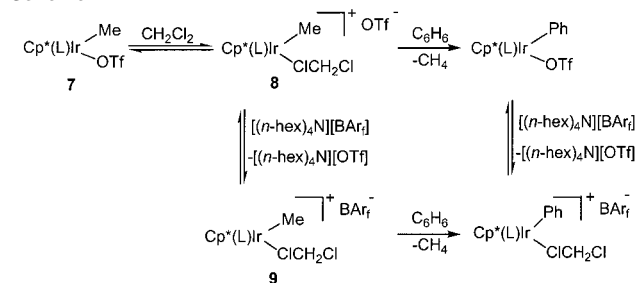


Figure 4. Plot of observed rate constant (k_{obs}) vs $[(n\text{-Hex})_4\text{NBAR}_f]$ for the reaction of **5** (0.013 M) and C_6H_6 (0.25 M) at 10 °C in CH_2Cl_2 .

Scheme 6



Scheme 7



salt approaches the rate of the BAR_f complexes **3** and **6** (e.g., for **6**, $k_{\text{obs}} = 3.4 \times 10^{-3} \text{ s}^{-1}$), but the complications at high salt concentrations prevented the observation of further approach toward this expected limit.

The increase in reaction rate for both the PMe_3 and the $\text{P}(\text{OMe})_3$ systems observed above demonstrates the operation of a salt effect. One explanation for this observation is that the added $(n\text{-Hex})_4\text{NBAR}_f$ directly assists in ionization of the triflate iridium bond (normal salt effect) (Scheme 6, complexes **1** and **5** are generalized as $\text{Cp}^*(\text{L})\text{IrMe}(\text{OTf})$ (**7**)).³⁴ Although normal salt effects on organic solvolysis reactions are not as large as those in polar solvents, rate increases of $>10^3$ have been seen in relatively nonpolar solvents such as diethyl ether and acetone.^{34,35}

However, our preferred rationale for this effect is that by introducing a source of borate anion, the iridium triflate complex **7** is activated by transiently forming a borate complex in solution. As depicted in Scheme 7, dissociation of the triflate anion from **7** produces ion pair **8**. Subsequent exchange between the triflate and BAR_f anions results in the BAR_f complex **9**. Both ion pairs **8** and **9** are assumed to react very rapidly and irreversibly with benzene. Yet with $(n\text{-Hex})_4\text{NBAR}_f$ salt, the equilibrium shifts toward the BAR_f complex **9** and away from the triflate ion pair **8** and its covalent complex **7** and, as a result, the reaction rate increases. This effect would be analogous to the special salt effect observed by Winstein and co-workers in the solvolysis reactions of alkylsulfonates in polar solvents (e.g.,

(33) Additionally, at such high salt concentrations the n -hexyl resonances of the added salt began to obscure the $\text{P}(\text{OMe})_3$ resonances, making the acquisition of reliable data difficult.

(34) Winstein, S.; Friedrich, E. C.; Smith, S. *J. Am. Chem. Soc.* **1964**, *86*, 305.

(35) For a theoretical treatment of salt effects in nonpolar solvents, see: Perrin, C. L.; Pressing, J. *J. Am. Chem. Soc.* **1971**, *93*, 5705.

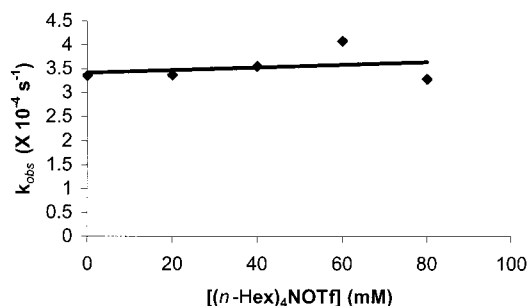


Figure 5. Plot of observed rate constant (k_{obs}) vs $[(n\text{-Hex})_4\text{NOTf}]$ for the reaction of **1** (1.1 mM) with 1.92 M C_6H_6 at 10 °C.

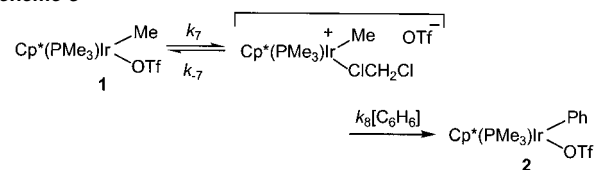
acetic acid) where addition of perchlorate anion results in a marked increase in the reaction rate.^{36–38} They attributed the rate increase to formation of a more reactive perchlorate species via exchange of the sulfonate anion for the perchlorate anion (analogous to our exchange of OTf for BAr_f).³⁹

When $(n\text{-Hex})_4\text{NBAR}_f$ is added to a mixture of the preformed phosphine CH_2Cl_2 /borate **3** and benzene, it does not affect the (already rapid) rate of reaction, nor is the reactivity of the phosphite CH_2Cl_2 /borate **6** affected by added $(n\text{-Hex})_4\text{NBAR}_f$. This result is consistent with our model since these CH_2Cl_2 /borate complexes already exist as ion pairs in solution, so there is no initial covalent–ionic preequilibrium in these systems that can be perturbed with added $(n\text{-Hex})_4\text{NBAR}_f$.^{8,40}

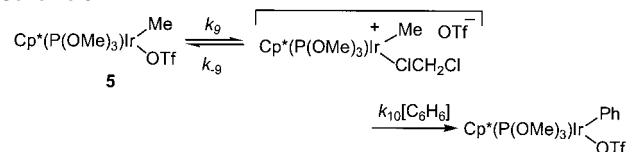
Qualitative reactivity studies of **1** with alkanes and ethers in the presence of $(n\text{-Hex})_4\text{NBAR}_f$ indicate that similar rate accelerations with added $(n\text{-Hex})_4\text{NBAR}_f$ salt occur for all substrates investigated. The increase in observed rate again spans almost 3 orders of magnitude upon the addition of $(n\text{-Hex})_4\text{NBAR}_f$. Such an extreme salt effect is likely a result of the stabilization of the ion pair by the highly polar added noncoordinating salts.³⁵

Effect of Added Triflate. When the reaction of triflate complex **1** with benzene was performed with variable amounts of added $(n\text{-Hex})_4\text{NOTf}$, the observed rate remained constant (Figure 5). This is not in agreement with preequilibration of **1** with free ions, which would predict an inverse dependence of k_{obs} on $[\text{OTf}]$ (Scheme 3, eq 3). The added $(n\text{-Hex})_4\text{NOTf}$ could also potentially serve to increase the effective solvent polarity and increase the rate of reaction. One explanation is that there are actually two counteracting effects: (a) inhibition of the ionization equilibrium by the common ion effect (as would be predicted from Scheme 1) and (b) a (fortuitously) compensating increase in the degree of ionization of **1** due to the increased effective polarity of the solution, thereby resulting in no net

Scheme 8



Scheme 9



change in the reaction rate.⁴¹ We believe it is highly unlikely that these effects would *exactly* cancel each other. Instead, it is more likely that $(n\text{-Hex})_4\text{NOTf}$ is also ion-paired and, as a result, does not change the ionic strength of the solvent significantly.^{42–45} In this scenario, no triflate inhibition is observed because benzene reacts directly with a tight or solvent-separated ion pair (Scheme 8, eq 5). This explanation is further supported by our observation that added PPNOTf also has no effect on the rate of benzene activation by phosphite **5** (Scheme 9, eq 6).⁴⁶

$$\text{rate} = k_{\text{obs}}[\mathbf{1}] = \frac{k_7 k_8 [\text{C}_6\text{H}_6]}{k_{-7} + k_8 [\text{C}_6\text{H}_6]} [\mathbf{1}] \quad (5)$$

$$\text{rate} = k_{\text{obs}}[\mathbf{5}] = \frac{k_9 k_{10} [\text{C}_6\text{H}_6]}{k_{-9} + k_{10} [\text{C}_6\text{H}_6]} [\mathbf{5}] \quad (6)$$

Solution Behavior of 1 and 3. In the solid state, complex **3** has a single chlorine-bound dichloromethane molecule coordinated to the iridium center. In CH_2Cl_2 solution, it is likely that a CH_2Cl_2 molecule would also occupy a coordination site of **3**. In CD_2Cl_2 solution, the CD_2Cl_2 /borate complex **3** shows discrete ^1H NMR chemical shifts clearly different from those assigned to the triflate analogue **1**. These large spectral differences are accounted for by our postulate that complex **1** exists predominantly as a covalent uncharged inner-sphere triflate, while complex **3** exists predominantly as a cationic covalent Ir– CH_2Cl_2 complex/borate ion pair.

Dichloromethane is a very weak donor ligand,¹⁷ and bound CH_2Cl_2 or CD_2Cl_2 likely undergoes rapid exchange with $\text{CD}_2\text{-Cl}_2$ solvent via a dynamic solvation equilibrium. Consistent with this assumption, at room temperature the ^1H NMR spectrum of a CD_2Cl_2 solution containing both the triflate complex **1** and the CD_2Cl_2 /borate salt **3** does not show resolved peaks for either compound. However, at lower temperatures the peaks

(36) Winstein, S.; Clippinger, E. J. *J. Am. Chem. Soc.* **1956**, *78*, 2784.

(37) Winstein, S.; Robinson, G. C. *J. Am. Chem. Soc.* **1958**, *80*, 169.

(38) Lowry, T. H.; Richardson, K. S. *Mechanism and Theory in Organic Chemistry*; Harper and Row: New York, 1987; Chapter 4.

(39) For the classical special salt effect observed with organic substrates in polar solvents, there is a large nonlinear increase in the rate constant at low salt concentrations. At higher salt concentrations, the rate constant growth slows down, becoming linear, similar to that observed for a normal salt effect. We believe we do not see a change in the slope of the plot for phosphine **1** because under our conditions, the special salt effect regime appears to extend to much higher concentrations of salt in the relatively nonpolar solvent CH_2Cl_2 .

(40) Recently, Johansson et al. have explored the reaction of diimine-based platinum cations with benzene in trifluoroethanol. In analogy to our results with **3**, they found that the addition of salts to the reaction mixture had no effect on the reaction rate. In addition, benzene coordination was found to be rate determining, and the C–H activation step most likely occurs via oxidative addition (Pt(II) to Pt(IV)). See ref 8.

(41) To probe this possibility further, an experiment was performed with **1** using variable ratios of $(n\text{-Hex})_4\text{NBAR}_f$ /($n\text{-Hex})_4\text{OTf}$ but with a constant total amount of salt ($(n\text{-Hex})_4\text{NBAR}_f + (n\text{-Hex})_4\text{NOTf} = \text{constant}$). While the results of these experiments did show inhibition at higher concentrations of triflate, the constant total salt concentration is a rather poor approximation for constant ion strength in dichloromethane, and the results cannot be quantitatively analyzed.

(42) For a discussion of the interactions between the PPN cation and different anions, see the two references immediately following this note.

(43) Tilset, M.; Zlota, A. A.; Folting, K.; Caulton, K. G. *J. Am. Chem. Soc.* **1993**, *115*, 4113.

(44) Alunni, S.; Pero, A.; Reichenbach, G. *J. Chem. Soc., Perkin Trans.* **1998**, 1747.

(45) See ref 29 for the observation of a relatively small linear salt effect in acetic acid solution with a common ion present.

(46) Consistent with this observation, compound **1** is a very weak electrolyte in CH_2Cl_2 . See ref 4.

for both compounds can be resolved ($T_c = -71$ °C, $\Delta G_c^\ddagger = 11.8$ kcal mol⁻¹).

Identities of the Reactive Species in CH₂Cl₂. We believe that the triflate complex **1** and the CD₂Cl₂/borate salt **3** lead to common or similar cationic Ir–CH₂Cl₂ intermediates. Two main pieces of evidence suggest that ion pairs (rather than free ions or the covalent triflate) are the reactive species in dichloromethane (Schemes 8 and 9). The first involves the lack of any common ion effect when (*n*-Hex)₄NOTf is added to the reaction mixture. This rules out the specific rate laws in eqs 3 and 4 which predict an inverse dependence on triflate concentration. The second piece of evidence stems from the fact that compound **5** reacts with benzene at a much slower rate than compound **1** does. The ion-pair mechanism illustrated in Scheme 8 predicts that a shift in the initial ionization equilibrium to the left (e.g., by replacing PMe₃ with P(OMe)₃) should slow the overall reaction rate. This also is consistent with our observations. In summary, the lack of a (*n*-Hex)₄NOTf dependence coupled with differences in reaction rates between **1** and **5** suggest that dissociation of triflate to generate a solvent-separated ion pair occurs prior to rate-limiting C–H activation.

Finally, it is important to ask whether the iridium cation reacts with benzene as the 18 e⁻ solvate or as the 16 e⁻ unsaturated cation; that is, does arene activation occur in a dissociative or an associative manner? We currently favor dissociative loss of dichloromethane prior to arene cleavage. This is based primarily upon results obtained with the hydridotris(pyrazolyl)borate (Tp) analogue of **3**, [Tp(PMe₃)Ir(Me)CH₂Cl₂][BAr_f], where we have evidence supporting the intermediacy of an unsaturated 16 e⁻ iridium cation.^{47,48} However, it should be noted that Gladysz and co-workers examined the mechanism of dichloromethane substitution in [CpPPh₃Re(NO)ClCH₂Cl][BF₄].⁴⁹ They concluded that the substitution likely occurred in an associative manner, via either an 18 e⁻ bent nitrosyl complex or, relevant to our system, an 18 e⁻ cyclopentadienyl slipped (η^3) complex. Recently, Tilset and Johansson have noted that the square planar cationic platinum complex [(diimine)PtCH₃(L)][OTf] activates C–H bonds in an associative manner.⁶ We are currently attempting to address this question with further studies on the Cp* system.

Reaction Trends Using Disubstituted Arenes as Substrates. The studies with added salt support the idea that the active iridium species in arene C–H activation is cationic and, therefore, possibly electrophilic. We decided to investigate whether the substrate's electronic properties would reflect this, predicting that electron-rich arenes should react faster. This was accomplished by comparing the rates of reaction of several 1,2-disubstituted arenes with complex **1**. We chose 1,2-disubstitution because most of these substrates react cleanly to yield a single product, resulting from attack at the 4-position of the arene (Scheme 10). 1,2-Difluorobenzene is an exception and yields two products, in about a 1:2 ratio. Characterization of this mixture by NMR spectroscopy indicates that they are the 1,2,3- and 1,3,4-trisubstituted products, respectively. In this case, it is postulated that the small size of the fluorine atom permits activation of the C–H bond at the 3-position.

Scheme 10

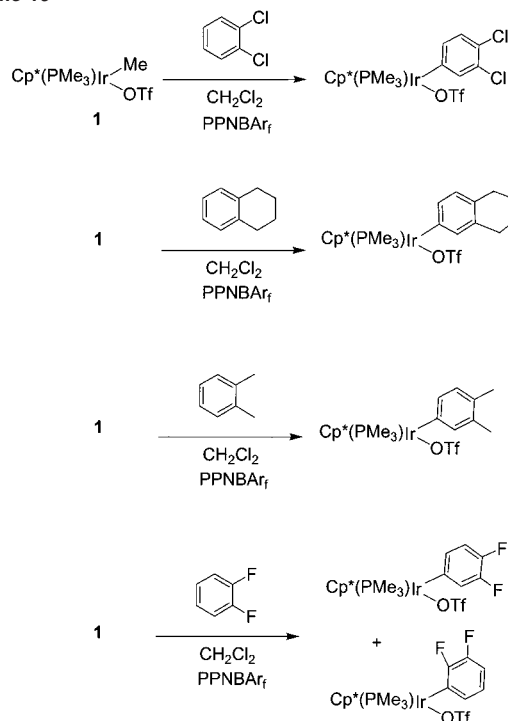


Table 1. Observed Rate Constants for the Reaction of **1** (1.90 mM) with 1,2-Disubstituted Arenes (51.2 mM) in CH₂Cl₂ at 14.1 °C^a

substrate	k_{obs} (s ⁻¹)
tetrahydronaphthalene	0.000844
xylene	0.001131
benzene ^b	0.000533
dichlorobenzene	0.000166

^a PPNBArf (20.0 mM) was also present. ^b Corrected for the number of hydrogens.

The observed rate constants for the reaction between **1** and the various substituted arenes are shown in Table 1. Benzene was statistically corrected by a factor of (2/6) due to the difference in the number of C–H bonds available for activation (six C–H bonds available on benzene vs two accessible C–H bonds on a disubstituted arene). While this system does not show completely linear Hammett-type behavior, there is a clear trend indicating that electron-withdrawing substituents decrease the reactivity of the substrate, as would be expected if the arene acts as a nucleophile.^{50,51}

A competition experiment carried out by treating a 10-fold excess 1:1 mixture of 1,2-dichlorobenzene and *o*-xylene with the CH₂Cl₂/borate complex **3** gave almost exclusively (>90% by NMR spectroscopy) the *o*-xylene activated product. This indicates that the CH₂Cl₂/borate complex **3**, like triflate complex **1**, also prefers electron-rich substrates.

Comparison of the Reactivity of the CH₂Cl₂/Borate Complexes **3 and **6**.** Interpretation of substituent effects at the metal center is complicated because modification of the complex has the potential to affect several different steps in the reaction

(47) Tellers, D. M.; Bergman, R. G. *Can. J. Chem.* **2001**, *79*, 525.

(48) Because **1** reacts quickly with benzene, and for solubility reasons, the reactions must be performed in dichloromethane, we have so far not been able to obtain experimental evidence supporting either mechanism.

(49) Dewey, M. A.; Zhou, Y.; Liu, Y.; Gladysz, J. A. *Organometallics* **1993**, *12*, 3924.

(50) Periana and co-workers have noted that methane bisulfate, the product of methane functionalization in their platinum system, is likely stable to overoxidation because of the electron-withdrawing character of the bisulfate group. See the following reference.

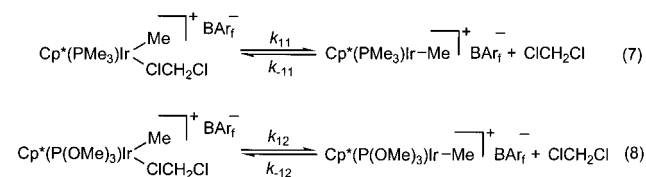
(51) Periana, R. A.; Taube, D. J.; Gamble, S.; Taube, H.; Satoh, T.; Fujii, H. *Science* **1998**, *280*, 560.

Table 2. Calculated Energies (kcal/mol) for the Reaction of [Cp(L)IrMe]⁺ with Methane^a

L = PMe ₃	energy (kcal/mol)	L = P(OMe) ₃	energy (kcal/mol)
[Cp(L)IrMe] ⁺ + CH ₄	0	[Cp(L)IrMe] ⁺ + CH ₄	0
[Cp(L)IrMe(H-CH ₃) ⁺	-0.3	[Cp(L)IrMe(H-CH ₃) ⁺	-3
[Cp(L)Ir(Me) ₂ H] ⁺	6.5	[Cp(L)Ir(Me) ₂ H] ⁺	4.8

^a Energy of “[Cp(L)IrMe]⁺ + methane” has been arbitrarily set to zero.

mechanism. For the triflate complexes **1** and **5**, both the initial preequilibrium step and the actual C–H bond activation step can be influenced by the electronic and steric differences caused by changes in electron density at the metal. While the preequilibrium effects were discussed earlier, we wished to determine the effect of such a substitution upon the actual C–H bond-breaking step. In an attempt to accomplish this, we compared the reactivity of the CH₂Cl₂/borate complexes **3** and **6**, where we know that dissociation of bound dichloromethane (*k*₁₁ in eq 7, *k*₁₂ in eq 8) is fast in both cases.



The reactions of the phosphine CH₂Cl₂/borate (**3**) and phosphite CH₂Cl₂/borate (**6**) complexes with benzene in CD₂-Cl₂ were both followed at 0 °C by NMR spectroscopy. These experiments showed that the phosphite complex (*k*_{obs} = (3.0 ± 0.3) × 10⁻⁴ s⁻¹) is less reactive than the phosphine complex (*k*_{obs} = (8.4 ± 0.8) × 10⁻³ s⁻¹) by a factor of nearly 30. Since the phosphite ligand is actually less sterically demanding than the phosphine ligand,⁵² this suggests that the diminished reactivity of the phosphite complex is due to an electronic rather than a steric effect, resulting from less electron density at the metal center. In parallel studies, we have found that replacing the Cp* ligand with the hydridotris(3,5-dimethylpyrazolyl)borate (Tp^{Me2}) ligand has given similar results.⁵³ The Tp^{Me2} ligand was shown to be less electron-donating than Cp*, and the resulting complex is less reactive than the Cp* complex **1**. However, in this case, it is more difficult to separate electronic from steric effects since the Tp^{Me2} ligand is also bulkier than the Cp* ligand.

It is tempting to attribute this effect to the C–H activation transition state. However, we believe that the more likely explanation is that decreasing the electron density at the metal center affects *k*₁₂/*k*₋₁₂ relative to *k*₁₁/*k*₋₁₁ (eqs 7 and 8); that is, the preequilibrium is shifted to the left, thereby decreasing the overall rate of C–H activation.⁴⁸ This explanation was reinforced by DFT calculations performed using Jaguar⁵⁴ at the B3LYP/LACVP**+ level of theory on the reaction of methane with the model system [Cp(L)IrMe]⁺ (L = PMe₃, P(OMe)₃). Optimized geometries and energies were calculated for [Cp(L)IrCH₃]⁺/CH₄, the alkane complex [Cp(L)IrCH₃(H-CH₃)⁺, and the iridium(V) complex [Cp(L)Ir(CH₃)₂H]⁺. The relative energies of these systems (Table 2) were in good accord with those reported by Hall and co-workers.¹¹ In both cases, as

expected, the alkane complex is somewhat lower in energy than the separated cation and free methane. Significantly, the alkane complex/oxidative addition product energy gap is very similar for the PMe₃ and P(OMe)₃ systems.⁵⁵ These calculations suggest that the rate difference observed between the phosphine **3** and phosphite **6** cannot be attributed solely to electronic differences in the C–H activation transition state.

Even if they are imprecise in an absolute sense, the results of the DFT calculations suggest it is likely that the rate difference between phosphine **3** and phosphite **6** is the result of the relative differences in dissociation of the dichloromethane ligand. Because the iridium center in phosphite **6** is less electron-rich, the rate of dissociation of dichloromethane is undoubtedly slower. This likely contributes to the slower rate of C–H activation by phosphite **6**. Overall, it is clear from this work that use of more electron-releasing ancillary ligands (i.e., phosphine vs phosphite) lowers the barrier to loss of the leaving group (OTf in **1**; CH₂Cl₂ in **3**) and, as a result, provides more facile access to the complex responsible for C–H activation.

Whatever the exact cause, it is clear that *the overall rate of C–H activation is inhibited by electron-withdrawing substituents on both the substrate and the complex*. This atypical pattern appears to contrast the standard “electrophile-nucleophile” pattern of reactivity that exists for most organic and organometallic even-electron bimolecular reactions.

Conclusion

The C–H activation reactions of triflate complex **1** with arene and alkane substrates almost certainly occur after dissociation of triflate, leading to a reactive cationic iridium/CH₂Cl₂ solvate (Scheme 8). The reaction is sensitive to medium effects; decreasing the effective polarity of the CH₂Cl₂ solvent by adding large amounts of benzene decreases the overall rate of reaction. Alternatively, the reactivity of **1** can be increased by almost 3 orders of magnitude by addition of the hydrophobic salt (*n*-Hex)₄NBAR_f. We believe that this is due to a special salt effect, with addition of salt causing triflate/BAR_f exchange and resulting in the formation of the more reactive iridium–borate ion pair.

Added salts are well known to increase the rates of ionic reactions in polar solvents.³¹ Quantitative studies of organometallic salt effects in nonpolar solvents are relatively rare, but salts have been used in several cases to increase rates or modify the nature of reactions in these media.³¹ This approach is advantageous because the system’s fundamental components remain unmodified chemically. In this regard, we are currently examining the activities of other organometallic reaction systems which involve ionic intermediates in nonpolar solvents with added bulky, soluble salts. As Winstein and co-workers noted in 1964, “Carrying out such [ionic organic] reactions under ‘salt promoted’ conditions may be useful practically and interesting theoretically.”³⁴

The reactions of **1** with 1,2-disubstituted arenes indicate that electron-withdrawing groups on the arene substrate decrease the reaction rates. The reactivity of the phosphite complex **5** was also compared to the reactivity of complex **1**. The relative reactivities of the phosphine and phosphite CH₂Cl₂/borate complexes indicate that electron-withdrawing groups on the

(52) Tolman, C. A. *Chem. Rev.* **1977**, *77*, 313.

(53) Tellers, D. M.; Bergman, R. G. *J. Am. Chem. Soc.* **2000**, *122*, 954.

(54) Jaguar, version 4.1; Schrödinger, Inc.: Portland, Oregon, 2000.

(55) The transition states were not sought for these two systems because it is unlikely that the relatively small difference in energy between the two systems would translate into a large energy difference in the transition state.

metal complex also decrease the *overall* rate.^{56–63} This unusual pattern of reactivity, whereby a reaction is enhanced by electron-withdrawing substituents on both reactants, is rather uncommon but may be reasonable considering the mechanism of C–H bond activation. We propose that this is caused by a decrease in the preequilibrium concentration of the reactive iridium cation. Additional work will be required on systems that are not complicated by an initial preequilibrium to conclusively identify the electron-density requirements of the metal center in so-called “electrophilic reactions”.

Finally, understanding the electronic requirements of C–H activation is potentially useful for gaining insight into the mechanism of C–H activation by other so-called “electrophilic” C–H activation reactions, such as those recently observed in analogous cationic platinum systems.^{8,9,20,51,64} A great deal of work has focused upon modeling the Shilov system³ by utilizing complexes of the type $[L_2PtMe(solvent)]^+$. To obtain a greater understanding of these systems and compare their behavior with that of the cationic Cp*- and Tp-substituted iridium systems, it would be useful to determine what electronic properties are important for both the substrate *and* the metal. Recent progress has been made on this problem;⁶⁵ as observed in our Ir system, the rate of C–H activation at platinum is also enhanced by increasing electron donation to the metal center.

Experimental Section

General. Unless otherwise noted, all reactions and manipulations were performed in a Vacuum Atmospheres circulating inert atmosphere glovebox or using standard Schlenk techniques. Glassware was dried in an oven at 150 °C before use. Unless otherwise noted, reagents were purchased from commercial suppliers and used without further purification. Merck silica gel, 60 Å, 230–400 mesh, grade 9385 was used in chromatography unless otherwise noted. Silated silica gel (Silica Gel 60), 63–200 μm particle size, was obtained from EM Science. Diethyl ether and THF were distilled from sodium/benzophenone ketyl under N₂ prior to use. Hexanes, pentane, benzene, and CH₂Cl₂ were passed through activated alumina under N₂, then sparged with N₂ and stored over 4 Å molecular sieves.⁶⁶ Deuterated solvents were degassed by freezing, evacuating, and thawing (3x), and were then dried over 4 Å sieves and stored under N₂.

Unless otherwise indicated, NMR spectra were obtained using a Bruker AMX-400 MHz spectrometer (400 MHz for ¹H spectra, 100.6 MHz for ¹³C{¹H} spectra, 162.1 MHz for ³¹P{¹H} spectra, 376.5 MHz for ¹⁹F spectra). Chemical shifts are reported in parts per million (δ) relative to residual protiated solvent, coupling constants are reported in Hertz (Hz), and integrations are reported in number of protons. Unless otherwise noted, samples for NMR analysis were prepared using CD₂-Cl₂ as the solvent.

- (56) See the seven references immediately following this note for studies of electronic effects on oxidative addition reactions.
 (57) Ugo, R.; Pasini, A.; Fusi, A.; Cennini, S. *J. Am. Chem. Soc.* **1972**, *94*, 7364.
 (58) Hascall, T.; Rabinovich, D.; Murphy, V. J.; Beachy, M. D.; Friesner, R. A.; Parkin, G. *J. Am. Chem. Soc.* **1999**, *121*, 11402.
 (59) Abu-Hasanayn, F.; Goldman, A. S.; Krogh-Jespersen, K. *J. Phys. Chem.* **1993**, *97*, 5890.
 (60) Sakaki, S.; Biswas, B.; Sugimoto, M. *Organometallics* **1998**, *17*, 1278.
 (61) van de Kuil, L. A.; Luitjes, H.; Grove, D. M.; Zwikker, J. W.; van der Linden, J. G. M.; Roelofs, A. M.; Jenneskens, L. W.; Drenth, W.; van Koten, G. *Organometallics* **1994**, *13*, 468.
 (62) Johnson, C. E.; Eisenberg, R. *J. Am. Chem. Soc.* **1985**, *107*, 3148.
 (63) Sargent, A. L.; Hall, M. B.; Guest, M. F. *J. Am. Chem. Soc.* **1992**, *114*, 517.
 (64) Fang, X.; Scott, B. L.; Watkin, J. G.; Kubas, G. *Organometallics* **2000**, *19*, 4193.
 (65) Zhong, H. A.; Labinger, J. A.; Bercaw, J. E. *J. Am. Chem. Soc.* **2002**, *124*, 1378–1399.
 (66) Alaimo, P. J.; Peters, D. W.; Arnold, J.; Bergman, R. G. *J. Chem. Educ.* **2001**, *78*, 64.

Kinetic studies were performed using a Hewlett-Packard 8453 UV–vis spectrometer or by NMR spectroscopy using a Bruker AMX-300 spectrometer (300 MHz for ¹H spectra) or a Bruker AMX-400 spectrometer (see above). All reaction mixtures were prepared under N₂ and kept under static N₂ during the kinetic analyses. For UV–vis kinetics experiments, the disappearance of **1** was monitored by change in absorbance at 314 nm. The disappearance of **5** was monitored at 300 nm. For NMR kinetics experiments, the disappearance of the Ir–Me resonances of **1** and **2** and the P(OMe)₃ resonances of **5** and **6** was monitored. Time versus absorbance data were plotted using Kaleidograph and fit to an exponential decay with a variable *t*_∞ value. Calibration of total sample volumes was done using a volumetric flask. The concentration versus absorption plots for complexes **1**, **2**, **5**, and **6** follow the Lambert–Beer law in CH₂Cl₂ for the concentration regimes studied (<5 mM).

Melting points were obtained with samples in sealed tubes under N₂ and are uncorrected. The compounds NaBARf,⁶⁷ PPNOTf,⁶⁸ [Cp*IrCl₂]₂,⁶⁹ Cp*(PMe₃)Ir(Cl)₂,⁶⁹ Cp*(PMe₃)Ir(OTf)₂,⁶⁹ Cp*(PMe₃)IrMe₂,⁴ and Cp*(PMe₃)IrMe(OTf)⁴ were prepared using literature procedures.

[(CH₃(CH₂)₅)₄N][B(3,5-C₆H₃(CF₃)₂)₄]. In a 20 mL scintillation vial containing 220 mg (0.57 mmol) of (*n*-Hex)₄NCl was added NaBARf (510 mg, 0.58 mmol) and CH₂Cl₂ (10 mL). The solution was stirred for 24 h, after which it was filtered through Celite, and the solvent was removed in vacuo. This provided (*n*-Hex)₄NBARf as a crude tan solid. The solid was dissolved in a minimum of CH₂Cl₂ (~1 mL), and pentane (~1 mL) was added. This mixture was cooled to –70 °C for 3 h, and the resulting clear, colorless crystals were removed by filtration and dried under vacuum. Recrystallization in an analogous manner yielded a white solid (370 mg, 75% yield). ¹H NMR (400 MHz, CD₂-Cl₂, 298 K): δ 7.72 (s, 8H, *o*-B(3,5-C₆H₃(CF₃)₂)₄), 7.55 (s, 4H, *p*-B(3,5-C₆H₃(CF₃)₂)₄), 3.03 (m, 8H, (CH₃(CH₂)₄CH₂)₄NH), 1.61 (m, 8H, (CH₃(CH₂)₃CH₂CH₂)₄N), 1.35 (m, 24H, (CH₃(CH₂)₃CH₂CH₂)₄N), 0.90 (t, 12H, ³J_{H–H} = 6.9 Hz, (CH₃(CH₂)₃CH₂CH₂)₄N). ¹³C{¹H} NMR (101 MHz, CD₂Cl₂, 298 K): δ 162.1 (q, ¹J_{B–C} = 50.1 Hz, *i*-B(Ar'₄)), 134.8 (m, *o*-B(Ar'₄)), 128.8 (q, ²J_{F–C} = 29.8 Hz, *m*-B(Ar'₄)), 124.9 (q, ¹J_{F–C} = 271.9 Hz, CF₃), 117.4 (septet, ³J_{F–C} = 4.0 Hz, *p*-B(Ar'₄)), 59.2 (s, (CH₃(CH₂)₄CH₂)₄N), 30.9 (s, (CH₃(CH₂)₃CH₂CH₂)₄N), 25.8 (s, (CH₃(CH₂)₂CH₂(CH₂)₂)₄N), 22.2 (s, (CH₃CH₂CH₂(CH₂)₃)₄N), 21.8 (s, (CH₃CH₂(CH₂)₄)₄N), 13.4 (s, (CH₃(CH₂)₂CH₂(CH₂)₂)₄N). ¹⁹F NMR (377 MHz, CD₂Cl₂, 298 K): –62.8 (s). Anal. Calcd for C₅₆H₇₆BF₂N: C, 54.68; H, 6.23; N, 1.14. Found: C, 54.76; H, 6.03; N, 1.13. mp 99–100 °C. UV–vis (CH₂Cl₂): λ_{max} = 308 nm, ε_{max} = 925 L mol^{–1} cm^{–1}.

[(CH₃(CH₂)₅)₄N][O₃SCF₃]. In a 20 mL scintillation vial containing 220 mg (0.56 mmol) of (*n*-Hex)₄NCl was added AgOTf (160 mg, 0.62 mmol) and CH₂Cl₂ (10 mL). The solution was stirred for 24 h in darkness, after which it was filtered through Celite, and the solvent was removed in vacuo over 1 day. This provided (*n*-Hex)₄NOTf as a clear, colorless liquid. The compound was cooled to –70 °C, and a white crystalline solid formed (280 mg, 99% yield). ¹H NMR (400 MHz, CD₂Cl₂, 298 K): δ 3.14 (m, 8H, (CH₃(CH₂)₄CH₂)₄N), 1.62 (m, 8H, (CH₃(CH₂)₃CH₂CH₂)₄N), 1.35 (m, 24H, (CH₃(CH₂)₃CH₂CH₂)₄N), 0.91 (t, 12H, ³J_{H–H} = 6.9 Hz, (CH₃(CH₂)₃CH₂CH₂)₄N). ¹³C{¹H} NMR (101 MHz, CD₂Cl₂, 298 K): δ 59.0 (s, (CH₃(CH₂)₄CH₂)₄N), 31.1 (s, (CH₃(CH₂)₃CH₂CH₂)₄N), 25.9 (s, (CH₃(CH₂)₂CH₂(CH₂)₂)₄N), 22.3 (s, (CH₃CH₂CH₂(CH₂)₃)₄N), 21.9 (s, (CH₃CH₂(CH₂)₄)₄N), 13.6 (s, (CH₃(CH₂)₂CH₂(CH₂)₂)₄N). ¹⁹F NMR (377 MHz, CD₂Cl₂, 298 K): δ –79 (s). Anal. Calcd for C₂₅H₅₂F₃N₃O₃S: C, 59.61; H, 10.40. Found: C, 59.63; H, 10.63. mp ~18 °C. UV–vis (CH₂Cl₂): λ_{max} = 308 nm, ε_{max} = 925 L mol^{–1} cm^{–1}.

[(PPh₃)₂N][3,5-C₆H₃(CF₃)₂]₄. In a 20 mL scintillation vial containing PPNCl (200 mg, 0.35 mmol) was added NaBARf (320 mg, 0.36 mmol) and CH₂Cl₂ (10 mL). The solution was stirred for 24 h, after

- (67) Brookhart, M.; Grant, B.; Volpe, A. F. *Organometallics* **1992**, *11*, 3920.
 (68) Obendorf, D.; Peringer, P. *Anorg. Chem. Org. Chem.* **1986**, *41*, 79.
 (69) Stang, P. J.; Huang, Y. H.; Arif, A. M. *Organometallics* **1992**, *11*, 231.

which it was filtered through Celite, and the solvent was removed in vacuo. This provided PPNBA_rf as a crude tan solid. The solid was dissolved in a minimum of CH₂Cl₂ (~1 mL), and pentane (~1 mL) was added. The mixture was cooled to -70 °C for 3 h, and the resulting white crystals were removed by filtration and dried. Recrystallization in an analogous manner yielded a white solid (370 mg, 75% yield). ¹H NMR (400 MHz, CDCl₃, 298 K): δ 7.71 (m, 8H, *o*-Ar'₄B), 7.59 (m, 6H, *p*-Ph₃P), 7.49 (s, 4H, *p*-Ar'₄B), 7.43 (m, 24H, *o*-Ph₃P). ¹³C{¹H} NMR (101 MHz, CDCl₃, 298 K): δ 162.3 (q, ¹J_{BC} = 50.1 Hz, *i*-B(Ar'₄)), 134.6 (s, *o*-B(Ar'₄)), 133.8 (s, *m*-PPH₃), 132.1 (d, *p*-PPH₃, ²J_{P-C} = 4.1 Hz), 129.5 (d, *o*-PPH₃, ³J_{P-C} = 4.1 Hz), 128.8 (q, ²J_{F-C} = 29.7 Hz, *m*-B(Ar'₄)), 124.9 (q, ¹J_{F-C} = 271.9 Hz, CF₃), 117.3 (septet, ³J_{F-C} = 3.8 Hz, *p*-B(Ar'₄)). ¹⁹F NMR (377 MHz, CDCl₃, 298 K): δ -62.5 (s). ³¹P{¹H} NMR (162 MHz, CD₂Cl₂, 298 K): 21.6 (s). Anal. Calcd for C₆₈H₄₂NBF₂P₂: C, 58.26; H, 3.02; N, 1.00. Found: C, 58.31; H, 2.98; N, 1.09. mp 170–172 °C. UV-vis (CH₂Cl₂): λ_{max} = 308 nm, ε_{max} = 925 L mol⁻¹ cm⁻¹.

Cp*(PMe₃)Ir(3,4-C₆H₃(CH₃)₂)OTf. The addition of 1,2-C₆H₄Me₂ (0.64 g, 6.0 mmol) to **1** (160 mg, 0.27 mmol) in CH₂Cl₂ (5 mL) resulted in the slow darkening of the reaction solution. After 24 h, the solvent was removed in vacuo to provide crude **12** as an orange solid. Crystallization from a mixture of pentane (~1 mL) and CH₂Cl₂ (~1 mL) at -70 °C led to **12** in 86% yield (160 mg, 0.23 mmol). ¹H NMR (400 MHz, CD₂Cl₂, 298 K): δ 6.9 (m, 3H, Ir-(3,4-C₆H₃Me₂)), 2.20 (s, 3H, Ir-(3,4-C₆H₃Me₂)), 2.16 (s, 3H, Ir-(3,4-C₆H₃Me₂)), 1.62 (d, 15H, ⁴J_{P-H} = 1.6 Hz, C₅Me₅), 1.45 (d, 9H, ²J_{P-H} = 10.7 Hz, PMe₃). ¹³C{¹H} NMR (101 MHz, CD₂Cl₂, 298 K): δ 133.8 (d, ³J_{P-C} = 3.1 Hz, *i*-C₆H₃Me₂), 128.1 (s, C₆H₃Me₂), 122.8 (s, C₆H₃Me₂), 122.1 (s, C₆H₃Me₂), 94.1 (s, C₅(Me)₅), 19.4 (s, C₆H₃Me₂), 18.5 (s, C₆H₃Me₂), 14.5 (d, ¹J_{P-C} = 50 Hz, PMe₃), 9.1 (s, C₅(Me)₅). ³¹P{¹H} NMR (162 MHz, CD₂Cl₂, 298 K): δ -23.6 (s). ¹⁹F NMR (377 MHz, CD₂Cl₂, 298 K): δ -78.7 (s). Anal. Calcd for C₂₂H₃₃F₃IrO₃PS: C, 40.17; H, 5.06. Found: C, 39.95; H, 4.76.

Cp*(PMe₃)Ir(C₆H₃(C₄H₈))OTf. The addition of 1,2,3,4-tetrahydronaphthalene (71 mg, 0.54 mmol) to **1** (61 mg, 0.11 mmol) in CH₂Cl₂ (5 mL) resulted in the slow darkening of the reaction solution. After 24 h, the solution was concentrated (1 mL) and passed through a plug of silted silica gel, making sure to collect only the orange band to obtain the product free of excess tetrahydronaphthalene. The resulting solution was concentrated in vacuo down to an orange foam which was rinsed with cold pentane (3 × 2 mL). The resulting solid was then extracted with pentane (4 × 5 mL). The light yellow pentane solution was concentrated (10 mL) and cooled to -40 °C. Orange crystals of Cp*(PMe₃)Ir(C₆H₃(C₄H₈)) (46 mg, 0.067 mmol) were isolated in 63% yield. ¹H NMR (500 MHz, CD₂Cl₂, 298 K): δ 6.92 (bm, 2H, C₆H₃(C₄H₈)), 6.75 (d, ²J_{H-H} = 7.5 Hz, 1H, C₆H₃(C₄H₈)), 2.73 (bs, 2H, C₆H₃(C₄H₈)), 2.67 (bs, 2H, C₆H₃(C₄H₈)), 1.73 (bs, 4H, C₆H₃(C₄H₈)), 1.65 (d, ⁴J_{P-H} = 1.5 Hz, 15H, C₅Me₅), 1.48 (d, ²J_{P-H} = 11 Hz, 9H, PMe₃). ¹³C{¹H} NMR (125 MHz, CD₂Cl₂, 298 K): δ 142.1 (d, ²J_{P-C} = 14 Hz, *i*-C₆H₃(C₄H₈)), 137.2 (s, C-H, C₆H₃(C₄H₈)), 136.7 (s, Cq, C₆H₃(C₄H₈)), 133.9 (s, C-H, C₆H₃(C₄H₈)), 131.4 (s, Cq, C₆H₃(C₄H₈)), 128.8 (s, C-H, C₆H₃(C₄H₈)), 93.6 (d, ²J_{P-C} = 4 Hz, C₅Me₅), 29.9 (s, C₆H₃(C₄H₈)), 29.2 (s, C₆H₃(C₄H₈)), 24.3 (s, C₆H₃(C₄H₈)), 24.3 (s, C₆H₃(C₄H₈)), 14.8 (d, ¹J_{P-C} = 37.8 Hz, PMe₃), 9.7 (s, C₅Me₅). ³¹P{¹H} NMR (162 MHz, CD₂Cl₂, 298 K): δ -22.4 (s). ¹⁹F NMR (377 MHz, CD₂Cl₂, 298 K): δ -77.1 (s). HRMS (EI) *m/z* for [C₂₄H₃₅O₃F₃PSIr]⁺ (M⁺): calcd 684.1626, obsd 684.1621. Anal. Calcd for C₂₄H₃₅F₃O₃PSIr⁺ (C₅H₁₂)_{0.5}: C, 44.22; H, 5.74. Found: C, 44.29; H, 5.70.

Cp*(PMe₃)Ir(C₆H₃Cl₂)OTf. Addition of 1,2-C₆H₄Cl₂ (370 mg, 2.5 mmol) to **1** (72 mg, 0.13 mmol) in CH₂Cl₂ (5 mL) resulted in the slow darkening of the reaction solution. After 24 h, the solvent was removed in vacuo to yield an orange solid. Crystallization from a mixture of pentane (~0.5 mL) and CH₂Cl₂ (~1 mL) at -30 °C led to Cp*(PMe₃)Ir(C₆H₃Cl₂)OTf in 48% yield (43 mg, 0.061 mmol). ¹H NMR (400 MHz, CD₂Cl₂, 298 K): δ 7.38 (bs, 1H, IrC₆H₃Cl₂), 7.14 (bm, 2H, IrC₆H₃Cl₂), 1.65 (d, ⁴J_{P-H} = 1.6 Hz, 15H, C₅Me₅), 1.50 (d, ²J_{P-H}

= 10.8 Hz, 9H, PMe₃). ¹³C{¹H} NMR (101 MHz, CD₂Cl₂, 298 K): δ 147.6 (d, ²J_{P-C} = 14 Hz, *i*-C₆H₃Cl₂), 137.8 (bs, *o*-C₆H₃Cl₂), 136.6 (bs, *o*-C₆H₃Cl₂), 131.7 (bs, C-Cl), 129.7 (s, *m*-C₆H₃Cl₂), 126.8 (s, C-Cl), 94.1 (d, ²J_{P-C} = 4 Hz, C₅Me₅), 14.7 (d, ¹J_{P-C} = 38 Hz, PMe₃), 9.7 (s, C₅Me₅). ³¹P{¹H} NMR (162 MHz, CD₂Cl₂, 298 K): δ -22.8. ¹⁹F NMR (377 MHz, CD₂Cl₂, 298 K): δ -77.0 (s). MS (EI) *m/z*: 698 (M⁺). Anal. Calcd for C₂₀H₂₇O₃IrPF₃Cl₂S: C, 34.39; H, 3.40. Found: C, 34.29; H, 3.76.

Cp*(PMe₃)Ir(3,4-C₆H₃F₂)OTf and Cp*(PMe₃)Ir(2,3-C₆H₃F₂)OTf. The addition of 1,2-C₆H₄F₂ (0.54 g, 4.7 mmol) to **1** (98 mg, 0.17 mmol) in 5 mL of CH₂Cl₂ resulted in the slow darkening of the reaction solution. After 24 h, the solvent was removed in vacuo to provide a mixture of isomers (ca. 1:2 ratio, with less than 5% impurities by ¹H NMR spectroscopy) as an orange solid in a 100% crude yield (120 mg, 0.17 mmol). The isomers could not be separated, and so the mixture was characterized only by ¹H and ¹⁹F NMR spectroscopy.

Major Isomer: ¹H NMR (400 MHz, CD₂Cl₂, 298 K): δ 7.0 (m, 3H, Ir-(3,4-C₆H₃F₂)), δ 1.64 (d, 15H, ⁴J_{P-H} = 1.5 Hz, C₅Me₅), δ 1.47 (d, 9H, ²J_{P-H} = 11.4 Hz, PMe₃). ³¹P{¹H} NMR (162 MHz, CD₂Cl₂, 298 K): δ -23.8 (s). ¹⁹F NMR (377 MHz, CD₂Cl₂, 298 K): δ -79 (s, OTf), δ -118 (s, C₆H₃F₂), δ -142 (s, C₆H₃F₂).

Minor Isomer: ¹H NMR (400 MHz, CD₂Cl₂, 298 K): δ 7.0 (m, 3H, Ir-(2,3-C₆H₃F₂)), 1.66 (d, 15H, ⁴J_{P-H} = 1.7 Hz, C₅Me₅), 1.54 (d, 9H, ²J_{P-H} = 11.7 Hz, PMe₃). ³¹P{¹H} NMR (162 MHz, CD₂Cl₂, 298 K): δ -24.0 (s). ¹⁹F NMR (377 MHz, CD₂Cl₂, 298 K): δ -78 (s, OTf), -141 (s, C₆H₃F₂), -149 (s, C₆H₃F₂).

Cp*(P(OMe)₃)Ir(Cl)₂. [Cp*IrCl₂]₂ (502 mg, 0.63 mmol) was dissolved in dry CH₂Cl₂ (120 mL) in a Schlenk flask with a stir bar. To this dark red solution was added P(OMe)₃ (0.20 g, 1.6 mmol), and the resulting mixture was allowed to stir under a static N₂ atmosphere for 2 h. The solvent was removed in vacuo providing a soft orange solid which was dissolved in CH₂Cl₂ and chromatographed in air on a short SiO₂ column (3 cm × 2 cm) using 75:25 Et₂O:CH₂Cl₂. The dark orange fraction was collected, and the solvent was removed in vacuo to provide Cp*(P(OMe)₃)Ir(Cl)₂ as a deep orange solid (605 mg, 92% yield). ¹H NMR (400 MHz, CD₂Cl₂, 298 K): δ 3.81 (d, ³J_{P-H} = 15.8 Hz, 6H, P(OMe)₃), 1.67 (d, ⁴J_{P-H} = 1.7 Hz, 15H, C₅Me₅). ¹³C{¹H} NMR (101 MHz, CD₂Cl₂, 298 K): δ 94.4 (s, C₅Me₅), 53.8 (s, P(OMe)₃), 8.34 (s, C₅Me₅). ³¹P{¹H} NMR (162 MHz, CD₂Cl₂, 298 K): δ 82.2 (s). Anal. Calcd for C₁₃H₂₄Cl₂IrO₃P: C, 29.89; H, 4.63. Found: C, 29.80; H, 4.63.

Cp*(P(OMe)₃)Ir(Me)₂. Cp*(P(OMe)₃)Ir(Cl)₂ (260 mg, 0.50 mmol) was suspended in THF (~14 mL) with stirring, and MeLi (~1.4 M in Et₂O, 1.0 mL) was added dropwise. Over 16 h, the solution turned light yellow. The solution was filtered through a medium porosity fritted funnel containing 3 g of alumina(III). The solids were washed with ~20 mL of additional Et₂O, and the yellow filtrates were collected and evaporated to dryness. The resulting yellow crystals were dissolved in pentane (20 mL) and passed through another fritted funnel containing 3 g of alumina(III), yielding a clear filtrate. The solvent was removed in vacuo, yielding white crystalline Cp*(P(OMe)₃)Ir(Me)₂ (130 mg, 56% yield). ¹H NMR (400 MHz, CD₂Cl₂, 298 K): δ 3.31 (d, ³J_{P-H} = 22 Hz, 9H, P(OMe)₃), 1.63 (d, ⁴J_{P-H} = 1.8 Hz, 15H, C₅Me₅), -0.04 (d, ³J_{P-H} = 5.2 Hz, 6H, IrMe₂). ¹³C{¹H} NMR (101 MHz, CD₂Cl₂, 298 K): δ 94.6 (s, C₅Me₅), 52.0 (s, P(OMe)₃), 9.87 (s, C₅Me₅), -19.4 (d, ²J_{P-C} = 10 Hz, Ir-Me₂). ³¹P{¹H} NMR (162 MHz, CD₂Cl₂, 298 K): δ 93.7 (s). Anal. Calcd for C₁₅H₃₀IrO₃P: C, 37.41; H, 6.28. Found: C, 37.42; H, 6.34.

Cp*(P(OMe)₃)Ir(OTf)₂. Cp*(P(OMe)₃)Ir(Cl)₂ (880 mg, 1.7 mmol) and AgOTf (410 mg, 3.4 mmol) were stirred in CH₂Cl₂ (~90 mL) under N₂ for 12 h in darkness. The solution was cannula filtered away from the off-white salts, and the orange supernatant was evaporated to dryness. The resulting bright orange solid was washed with ether (3 × 15 mL) to remove trace Ag-containing impurities, and the solids remaining were dried under vacuum to yield Cp*(P(OMe)₃)Ir(OTf)₂ (1.2 g, 92% yield). Material suitable for elemental analysis was obtained

by crystallization at $-40\text{ }^{\circ}\text{C}$ from a concentrated CH_2Cl_2 solution layered with pentane. ^1H NMR (400 MHz, CD_2Cl_2 , 298 K): δ 3.84 (d, 6H, $^3J_{\text{P-H}} = 12.4\text{ Hz}$, $\text{P}(\text{OMe})_3$), 1.63 (d, 15H, $^4J_{\text{P-H}} = 3.1\text{ Hz}$, C_5Me_5). $^{13}\text{C}\{^1\text{H}\}$ NMR (99.7 MHz, CD_2Cl_2 , 298 K): δ 94.9 (s, C_5Me_5), 53.2 (s, $\text{P}(\text{OMe})_3$), 9.30 (s, C_5Me_5). $^{31}\text{P}\{^1\text{H}\}$ NMR (162 MHz, CD_2Cl_2 , 298 K): δ 107.3 (s). ^{19}F NMR (377 MHz, CD_2Cl_2 , 298 K): δ -78.9 (s, OTf). MS (EI): m/z 750 (M^+). Anal. Calcd for $\text{C}_{15}\text{H}_{24}\text{F}_6\text{IrO}_9\text{PS}_2$: C, 37.41; H, 6.28. Found: C, 37.42; H, 6.34.

$\text{Cp}^*(\text{P}(\text{OMe})_3)\text{IrMe}(\text{OTf})$ (5). A diethyl ether (200 mL) solution of $\text{Cp}^*(\text{P}(\text{OMe})_3)\text{IrMe}_2$ (3.2 g, 6.4 mmol) was added to a 500 mL round-bottom flask containing $\text{Cp}^*(\text{P}(\text{OMe})_3)\text{Ir}(\text{OTf})_2$ (4.8 g, 6.4 mmol). Upon stirring for 1 day, all of the material had dissolved. The orange solution was filtered through silylated silica gel, washed with diethyl ether, and the solvent was removed in vacuo. The orange solid was washed with pentane (50 mL) and dried in vacuo to afford **5** (7.3 g, 93% yield). ^1H NMR (400 MHz, CD_2Cl_2 , 298 K): δ 3.74 (d, $^3J_{\text{P-H}} = 11.5\text{ Hz}$, 6H, $\text{P}(\text{OMe})_3$), 1.73 (d, $^4J_{\text{P-H}} = 3.2\text{ Hz}$, 15H, C_5Me_5), 1.20 (d, $^3J_{\text{P-H}} = 6.5\text{ Hz}$, 3H, Ir-Me). $^{13}\text{C}\{^1\text{H}\}$ NMR (101 MHz, CD_2Cl_2 , 298 K): δ 94.9 (s, C_5Me_5), 52.5 (s, $\text{P}(\text{OMe})_3$), 9.92 (s, C_5Me_5), -11.4 (s, Ir-Me). $^{31}\text{P}\{^1\text{H}\}$ NMR (162 MHz, CD_2Cl_2 , 298 K): δ 97.5 (s). ^{19}F NMR (377 MHz, CD_2Cl_2 , 298 K): δ -78.6 (s). Anal. Calcd for $\text{C}_{15}\text{H}_{27}\text{F}_3\text{IrO}_6\text{PS}$: C, 29.27; H, 4.42. Found: C, 29.24; H, 4.56.

$\text{Cp}^*(\text{P}(\text{OMe})_3)\text{IrPh}(\text{OTf})$. The addition of C_6H_6 (1.0 g, 13 mmol) to **5** (230 mg, 0.370 mmol) in 7 mL of CH_2Cl_2 resulted in the darkening of the reaction solution over 2 h. After 10 h, the solvent was removed in vacuo to provide $\text{Cp}^*(\text{P}(\text{OMe})_3)\text{IrPh}(\text{OTf})$ as an orange solid (250 mg, 99% yield). ^1H NMR (400 MHz, CD_2Cl_2 , 298 K): δ 7.64 (d, $^2J_{\text{H-H}} = 7.4\text{ Hz}$, 2H, *o*- C_6H_5), 7.30 (dd, $^3J_{\text{H-H}} = 7.4$ and 7.6 Hz , 2H, *m*- C_6H_5), 7.08 (t, $^3J_{\text{H-H}} = 7.6\text{ Hz}$, 1H, *p*- C_6H_5), 3.67 (d, $^2J_{\text{P-H}} = 11.2\text{ Hz}$, 9H, $\text{P}(\text{OMe})_3$), δ 1.74 (d, $^4J_{\text{P-H}} = 2.7\text{ Hz}$, 15H, C_5Me_5). $^{13}\text{C}\{^1\text{H}\}$ NMR (101 MHz, CD_2Cl_2 , 298 K): δ 140.1 (d, $^2J_{\text{P-C}} = 15.3\text{ Hz}$, *i*- C_6H_5), 130.7 (s, *o*- C_6H_5), 128.0 (s, *m*- C_6H_5), 123.2 (s, *p*- C_6H_5), 96.1 (s, C_5Me_5), 52.5 (s, $\text{P}(\text{OMe})_3$), 8.94 (s, C_5Me_5). $^{31}\text{P}\{^1\text{H}\}$ NMR (162 MHz, CD_2Cl_2 , 298 K): δ 94.2 (s). ^{19}F NMR (377 MHz, CD_2Cl_2 , 298 K): δ -78.5 (s). HRMS (EI) m/z for $[\text{C}_{20}\text{H}_{29}\text{O}_6\text{F}_3\text{PSIr}]^+$ (M^+): calcd 678.1004, obsd 678.1006.

$[\text{Cp}^*(\text{P}(\text{OMe})_3)\text{Ir}(\text{Me})\text{CD}_2\text{Cl}_2][\text{BARf}]$ (6). In a glovebox, complex **5** (10 mg, 0.016 mmol) was dissolved in CD_2Cl_2 (2 mL) and cooled to $-40\text{ }^{\circ}\text{C}$ before NaBARf (14 mg, 0.016 mmol) was added, and the mixture was shaken intermittently over 5 min at $-40\text{ }^{\circ}\text{C}$. The mixture was then filtered through a precooled glass wool plug, and the solution of **6** was used directly for kinetic experiments or characterization. Removal of the solvent leads to degradation of **6**. ^1H NMR (400 MHz, CD_2Cl_2 , 298 K): δ 7.72 (s, 8H, *o*- $\text{Ar}'_4\text{B}$), 7.57 (s, 4H, *p*- $\text{Ar}'_4\text{B}$), 3.74 (d, $^3J_{\text{P-H}} = 11.5\text{ Hz}$, 6H, $\text{P}(\text{OMe})_3$), 1.71 (d, $^4J_{\text{P-H}} = 2.9\text{ Hz}$, 15H, C_5Me_5), 1.15 (d, $^3J_{\text{P-H}} = 4.8\text{ Hz}$, 3H, Ir-Me). $^{31}\text{P}\{^1\text{H}\}$ NMR (162 MHz, CD_2Cl_2 , 298 K): δ 87.1 (s). ^{19}F NMR (377 MHz, CD_2Cl_2 , 298 K): δ -62.9 (s).

$[\text{Cp}^*(\text{P}(\text{OMe})_3)\text{Ir}(\text{Ph})\text{CD}_2\text{Cl}_2][\text{BARf}]$. Method A: To a $-40\text{ }^{\circ}\text{C}$ solution of **6** (6.4 mg, 0.010 mmol) in CD_2Cl_2 (0.6 mL) was added C_6H_6 (8.1 mg, 0.10 mmol). The solution was allowed to warm to room temperature, and after 20 min ^1H NMR spectroscopy indicated that complete conversion to $[\text{Cp}^*(\text{P}(\text{OMe})_3)\text{Ir}(\text{Ph})\text{CD}_2\text{Cl}_2][\text{BARf}]$ had occurred. As with compound **6**, attempts to isolate $[\text{Cp}^*(\text{P}(\text{OMe})_3)\text{Ir}(\text{Ph})\text{CD}_2\text{Cl}_2][\text{BARf}]$ were unsuccessful.

Method B: To a solution of $\text{Cp}^*(\text{P}(\text{OMe})_3)\text{IrPh}(\text{OTf})$ (7.1 mg, 0.010 mmol) in CD_2Cl_2 (0.5 mL) was added a slurry of NaBARf (9.3 mg, 0.010 mmol) in CD_2Cl_2 (0.5 mL). The solution was shaken for 10 min and transferred to a NMR tube. Complete conversion to $[\text{Cp}^*(\text{P}(\text{OMe})_3)\text{Ir}(\text{Ph})\text{CD}_2\text{Cl}_2][\text{BARf}]$ was observed as determined by ^1H NMR spectroscopy. ^1H NMR (400 MHz, CD_2Cl_2 , 298 K): δ 7.76 (s, 8H, *o*- $\text{Ar}'_4\text{B}$), 7.59 (s, 4H, *p*- $\text{Ar}'_4\text{B}$), 7.25 (d, $^3J_{\text{H-H}} = 7.6\text{ Hz}$, 2H, *o*- C_6H_5), 7.14 (t, $^3J_{\text{H-H}} = 7.1\text{ Hz}$, 2H, *m*- C_6H_5), 7.02 (t, $^3J_{\text{H-H}} = 7.2\text{ Hz}$, 1H, *p*- C_6H_5), 3.73 (d, 6H, $^3J_{\text{P-H}} = 11.3\text{ Hz}$, $\text{P}(\text{OMe})_3$), 1.59 (d, 15H, $^4J_{\text{P-H}} = 2.8\text{ Hz}$, C_5Me_5). $^{31}\text{P}\{^1\text{H}\}$ NMR (162 MHz, CD_2Cl_2 , 298 K): δ 82.8 (bs). ^{19}F NMR (377 MHz, CD_2Cl_2 , 298 K): δ -62.9 (s).

Kinetics of Conversion of 1 and C_6H_6 to 2. A typical experiment was performed as follows. In a glovebox, **1** (6.1 mg, 0.011 mmol) was dissolved in CH_2Cl_2 (1 mL) and added to a 10 mL volumetric flask. To this was added a CH_2Cl_2 (6 mL) solution of PPNOTf (12.0 mg, 0.018 mmol) and benzene (3.1 g, 0.039 mol). The solution was diluted to 10 mL with CH_2Cl_2 . The solution was stirred briefly and then transferred ($\sim 4\text{ mL}$) by pipet to a quartz UV-vis cuvette equipped with a Kontes high-vacuum Teflon stopcock. The cuvette was removed from the box and immediately placed at $10.0\text{ }^{\circ}\text{C}$ in the UV-vis cuvette holder. Spectra were acquired at 300 s intervals over 8 h.

Kinetics of Conversion of 5 and C_6H_6 to $\text{Cp}^*(\text{P}(\text{OMe})_3)\text{IrPh}(\text{OTf})$. A typical experiment was performed as follows. In a glovebox, a 2 mL volumetric flask was charged with hexamethylbenzene (2.2 mg, 0.014 mmol), C_6H_6 (180 μL , 2.01 mmol), and diluted to 2 mL with CD_2Cl_2 . A 1 mL volumetric flask was charged with **5** (8.0 mg, 0.013 mmol) and diluted to 1 mL with the benzene/ CD_2Cl_2 solution. The orange solution was mixed thoroughly and then transferred to an NMR tube. The tube was attached to a Cajon adapter, degassed on a vacuum line, and flame sealed. The tube was kept at $-196\text{ }^{\circ}\text{C}$ until it was ready to be placed in an NMR probe held at $30 \pm 0.1\text{ }^{\circ}\text{C}$. Spectra were acquired at 300 s intervals over 10 h.

Kinetic Experiments on the Reaction of 1 with Benzene in the Presence of Added $[(\text{CH}_3(\text{CH}_2)_5)_4\text{N}][\text{B}(3,5\text{-C}_6\text{H}_3(\text{CF}_3)_2)_4]$. A typical experiment was performed as follows. In a glovebox, 16.2 mg (0.0284 mmol) of **1** was dissolved in CH_2Cl_2 and added to a 10 mL volumetric flask. The solution was diluted to 10 mL with CH_2Cl_2 . An aliquot of the resulting solution (1.00 mL) was transferred to a 20 mL scintillation vial containing 1.0 mL of a CH_2Cl_2 solution of $[(n\text{-hexyl})_4\text{N}][\text{BARf}]$ (115 mg, 0.094 mmol). Also transferred to the vial was 1.00 mL of a 0.154 M solution of C_6H_6 in CH_2Cl_2 . The solution was stirred briefly to ensure the salt was completely dissolved, and it was then transferred by pipet to a quartz UV-vis cuvette equipped with a Kontes high-vacuum Teflon stopcock. The cuvette was removed from the box and immediately placed at $14.1\text{ }^{\circ}\text{C}$ in the UV-vis cuvette holder. Spectra were acquired at 100 s intervals over 4 h.

Kinetic Experiments on the Reaction of 5 with Benzene in the Presence of Added $[(\text{CH}_3(\text{CH}_2)_5)_4\text{N}][\text{B}(3,5\text{-C}_6\text{H}_3(\text{CF}_3)_2)_4]$. A typical experiment was performed as follows. A vial was charged with **5** (8.0 mg, 0.013 mmol) and 0.5 mL of CD_2Cl_2 to yield an orange solution. A second vial was charged with 0.5 mL of CD_2Cl_2 , C_6H_6 (0.9 mg, 0.006 mmol), C_6H_6 (23 μL , 0.25 mmol), and $(n\text{-hexyl})_4\text{NBARf}$ (24 mg, 0.020 mmol) to yield a clear solution. This clear solution was added to the orange solution of **5** and mixed thoroughly. The mixture was transferred to an NMR tube using a pipet. The tube was attached to a Cajon adapter, degassed on a vacuum line, and flame sealed. The tube was kept at $-196\text{ }^{\circ}\text{C}$ until it was ready to be placed in an NMR probe held at $30 \pm 0.1\text{ }^{\circ}\text{C}$. Spectra were acquired at 300 s intervals over 10 h.

Examination of Triflate Dependence for the Reaction of 1 with Benzene. A typical experiment was performed as follows. In a glovebox, **1** (6.1 mg, 0.011 mmol) was dissolved in CH_2Cl_2 (4 mL) and added to a 10 mL volumetric flask. To this was added a CH_2Cl_2 (4 mL) solution of $(n\text{-Hex})_4\text{NOTf}$ (101 mg, 0.200 mmol) and benzene (1.5 g, 0.019 mol). The solution was diluted to 10 mL with CH_2Cl_2 . The solution was stirred briefly and then transferred ($\sim 4\text{ mL}$) by pipet to a quartz UV-vis cuvette equipped with a Kontes high-vacuum Teflon stopcock. The cuvette was removed from the box and immediately placed at $10.0\text{ }^{\circ}\text{C}$ in the UV-vis cuvette holder. Spectra were acquired at 300 s intervals over 8 h.

Examination of Triflate Dependence for the Reaction of 5 with Benzene. To a vial containing **5** (8.7 mg, 0.014 mmol) was added a $-40\text{ }^{\circ}\text{C}$ solution of C_6H_6 (0.10 mL, 1.1 mmol) in CD_2Cl_2 (0.65 mL, $[\text{Ir}] = 0.019\text{ M}$, $[\text{C}_6\text{H}_6] = 1.5\text{ M}$). This solution was kept at $-40\text{ }^{\circ}\text{C}$ while a second vial containing **5** (8.3 mg, 0.014 mmol) was charged with a $-40\text{ }^{\circ}\text{C}$ solution of C_6H_6 (0.10 mL, 1.1 mmol) and PPNOTf (9.3 mg, 0.014 mmol) in CD_2Cl_2 (0.65 mL, $[\text{Ir}] = 0.018\text{ M}$, $[\text{C}_6\text{H}_6] = 1.5\text{ M}$, $[\text{PPNOTf}] = 0.019\text{ M}$). Upon mixing of this second reaction,

each solution was transferred to a separate NMR tube and allowed to warm to room temperature. The reactions were monitored by ^1H NMR spectroscopy until all of **5** had been consumed (8 h). Each reaction had a $t_{1/2} = 1.5$ h.

Kinetic Experiments on 1 with 1,2-Disubstituted Arenes. A typical experiment was performed as follows. In a glovebox, 16.2 mg (0.0284 mmol) of **1** was dissolved in CH_2Cl_2 and added to a 10 mL volumetric flask. The solution was diluted to 10.0 mL with CH_2Cl_2 . A volume of 2.00 mL of this solution was transferred to a 20 mL scintillation vial containing 1.00 mL of a 0.154 M stock solution of $\text{C}_6\text{H}_4\text{Cl}_2$ in CH_2Cl_2 . The solution was stirred briefly to ensure complete mixing and was then transferred by pipet to a quartz UV-vis cuvette equipped with a Kontes high-vacuum Teflon stopcock. The cell was removed from the glovebox and immediately placed at 14.1 °C in the UV-vis cuvette holder. Spectra were acquired at 200 s intervals over 12 h.

Competition Experiments of 3 or 6 with 1,2-Disubstituted Arenes. A typical experiment was performed as follows. To 0.5 mL of a CD_2Cl_2 solution of 150 mM 1,2-dichlorobenzene and 150 mM *o*-xylene was added 0.5 mL of a freshly prepared solution of **6** in CD_2Cl_2 (approximately 8.0 mM). The resulting mixture was sealed and allowed to sit for 5 h at room temperature. The resulting products were analyzed by $^{31}\text{P}\{^1\text{H}\}$ NMR spectroscopy and compared to the spectra of the corresponding single-substrate reaction products.

Kinetic Experiments on the Reactions of 3 and 6 with Benzene. A typical experiment was performed as follows. To 0.5 mL of a CD_2Cl_2 solution of 0.26 M benzene and C_6Me_6 (0.9 mg, 0.006 mmol) at -40 °C was added 0.5 mL of a freshly prepared solution of **5** in CD_2Cl_2 (approximately 26 mM) at -40 °C. The solution was mixed thoroughly to yield an orange solution (13 mM **5**, 0.13 M C_6H_6), which was transferred to an NMR tube. The tube was attached to a Cajon adapter, degassed on a vacuum line, and flame sealed. The tube was kept at -196 °C until it was ready to be placed in an NMR probe held at 30 ± 0.1 °C. Spectra of **6** were acquired at 300 s intervals over 10 h, and spectra **3** were acquired at 12 s intervals over 15 min.

DFT Calculations. Geometries were calculated with density functional theory using the B3LYP functional and the LACVP**+ basis set in Jaguar.⁵⁴ Calculations were performed using Jaguar 4.0⁵⁴ on either Pentium Coppermine or AMD Athlon-based PCs running Redhat Linux 6.2 and openPBS.⁷⁰ Molden was used for visualization of results.⁷¹ The

B3LYP functional uses Becke's three-parameter exchange functional⁷² with the LYP nonlocal correlation functional.⁷³ The LACVP basis set⁷⁴ uses the Pople 6-31 bases⁷⁵ for H-Ar. Iridium is represented using the outermost core orbitals and the Los Alamos effective core potentials.^{76,77} A single asterisk (*) indicates the addition of polarization functions to carbon and phosphorus; double asterisks (**) indicate the addition of polarization functions to hydrogen, carbon, and phosphorus. Likewise, a single plus (+) indicates the addition of diffuse functions to carbon and phosphorus. The energies obtained do not take into account zero-point or Gibbs energies and are therefore reported as free energies, ΔE .

Acknowledgment. This work was supported by the Director, Office of Energy Research, Office of Basic Energy Sciences, Chemical Sciences Division, U.S. Department of Energy, under Contract No. DE-AC03-76SF00098. We acknowledge Boehringer-Ingelheim Pharmaceuticals, Inc. for a graduate fellowship (D.M.T.). We would also like to thank Drs. Andrew Streitwieser, Charles Perrin, Joseph Gajewski, and J. Robin Fulton for helpful discussions, Dr. Bernd Straub for assistance with DFT calculations, and Drs. John Bercaw and Jay Labinger for helpful discussions and disclosure of results prior to publication.

Supporting Information Available: Tables containing the kinetic data illustrated in Figures 1, 2, 3, 4, and 5 (PDF). This material is available free of charge via the Internet at <http://pubs.acs.org>.

JA011809U

(70) *OpenPBS*, version 2.3.1; Veridian Systems: Mountain View, California, 2000.

(71) Schaftenaar, G.; Noordik, J. H. *J. Comput.-Aided Mol. Des.* **2000**, *14*, 123.

(72) Becke, A. D. *J. Chem. Phys.* **1993**, *98*, 5648.

(73) Lee, C.; Yang, W.; Parr, R. G. *Phys. Rev. B* **1988**, *37*, 785.

(74) Hay, P. J.; Wadt, W. R. *J. Chem. Phys.* **1985**, *82*, 299.

(75) Frisch, M. J.; Pople, J. A.; Binkley, J. S. *J. Chem. Phys.* **1984**, *80*, 3265.

(76) Hay, P. J.; Wadt, W. R. *J. Chem. Phys.* **1985**, *82*, 270.

(77) Hay, P. J.; Wadt, W. R. *J. Chem. Phys.* **1985**, *82*, 284.